Research Article | Vol. 8, No. 11 | 1 Nov 2017 | BIOMEDICAL OPTICS EXPRESS 5191
Biomedical Optics EXPRESS

Label-free fiber optic optrode for the detection of class C β-lactamases expressed by drug resistant bacteria

Simona Zuppolini,[1,7] Giuseppe Quero,[2,7] Marco Consales,[2] Laura Diodato,[1] Patrizio Vaiano,[2] Alberto Venturelli,[3] Matteo Santucci,[4] Francesca Spyrakis,[4,5] Maria P. Costi,[4] Michele Giordano,[6] Antonello Cutolo,[2] Andrea Cusano,[2,8] and Anna Borriello[1,9]

[1]*Institute for Polymers, Composites and Biomaterials - National Council of Research, Portici, Italy*
[2]*Optoelectronics Group, Dept. of Engineering, University of Sannio, Benevento, Italy*
[3]*Tydock Pharma S.r.l, Modena, Italy*
[4]*Dept. of Life Sciences, University of Modena and Reggio Emilia, Modena, Italy*
[5]*Current Address: Dept. of Drug Science and Technology, University of Torino, Torino, Italy*
[6]*Optosmart S.r.l., Portici, Italy*
[7]*These authors contributed equally to this work*
[8]*a.cusano@unisannio.it*
[9]*borriell@unina.it*

Abstract: This paper reports the experimental assessment of an automated optical assay based on label free optical fiber optrodes for the fast detection of class C β-lactamases (AmpC BLs), actually considered as one of the most important sources of resistance to β-lactams antibiotics expressed by resistant bacteria. Reflection-type long period fiber gratings (RT-LPG) have been used as highly sensitive label free optrodes, while a higher affine boronic acid-based ligand was here selected to enhance the overall assay performances compared to those obtained in our first demonstration. In order to prove the feasibility analysis towards a fully automated optical assay, an engineered system was developed to simultaneously manipulate and interrogate multiple fiber optic optrodes in the different phases of the assay. The automated system tested in AmpC solutions at increasing concentrations demonstrated a limit of detection (LOD) of 6 nM, three times better when compared with the results obtained in our previous work. Moreover, the real effectiveness of the proposed optical assay has been also confirmed in complex matrices as the case of lysates of Escherichia coli overexpressing AmpC.

OCIS codes: (280.1415) Biological sensing and sensors; (060.2390) Fiber optic, infrared; (170.4580) Optical diagnostics for medicine; (230.4170) Multilayers; (350.2770) Gratings

References and links

1. D. Farina, F. Spyrakis, A. Venturelli, S. Cross, D. Tondi, and M. P. Costi, "The inhibition of extended spectrum β-lactamases: hits and leads," Curr. Med. Chem. **21**(12), 1405–1434 (2014).
2. H. Nikaido, "Multidrug Resistance in Bacteria," Annu. Rev. Biochem. **78**(1), 119–146 (2009).
3. F. Spyrakis, "Editorial Thematic issue: from extended spectrum β-lactamases to carbapenemase: the never ending challenge against gram-negative bacteria," Curr. Drug Targets **17**(9), 972–973 (2016).
4. A. Venturelli, D. Tondi, L. Cancian, F. Morandi, G. Cannazza, B. Segatore, F. Prati, G. Amicosante, B. K. Shoichet, and M. P. Costi, "Optimizing cell permeation of an antibiotic resistance inhibitor for improved efficacy," J. Med. Chem. **50**(23), 5644–5654 (2007).
5. D. Tondi, S. Cross, A. Venturelli, M. P. Costi, G. Cruciani, and F. Spyrakis, "Decoding the structural basis for carbapenem hydrolysis by class A β-lactamases: fishing for a pharmacophore," Curr. Drug Targets **17**(9), 983–1005 (2016).
6. C. G. Carvalhaes, R. C. Picao, A. G. Nicoletti, D. E. Xavier, and A. C. Gales, "Cloverleaf test (modified Hodge test) for detecting carbapenemase production in *Klebsiella pneumoniae*: be aware of false positive results," J. Antimicrob. Chemother. **65**(2), 249–251 (2010).

#300902 https://doi.org/10.1364/BOE.8.005191
Journal © 2017 Received 27 Jun 2017; revised 24 Aug 2017; accepted 24 Aug 2017; published 23 Oct 2017
Corrected: 26 October 2017

Biomedical Optics EXPRESS

7. J. Hrabak, E. Chudackova, and C. C. Papagiannitsis, "Detection of carbapenemases in *Enterobacteriaceae*: a challenge for diagnostic microbiological laboratories," Clin. Microbiol. Infect. **20**(9), 839–853 (2014).
8. K. Lee, Y. Chong, H. B. Shin, Y. A. Kim, D. Yong, and J. H. Yum, "Modified Hodge and EDTA-disk synergy tests to screen metallo-β-lactamase-producing strains of pseudomonas and acinetobacter species," Clin. Microbiol. Infect. **7**(2), 88–91 (2001).
9. P. Nordmann, M. Gniadkowski, C. G. Giske, L. Poirel, N. Woodford, and V. Miriagou, "Identification and screening of carbapenemase-producing *Enterobacteriaceae*," Clin. Microbiol. Infect. **18**(5), 432–438 (2012).
10. C. Ratkai, S. Quinteira, F. Grosso, N. Monteiro, E. Nagy, and L. Peixe, "Controlling for false positives: interpreting MBL Etest and MBL combined disc test for the detection of metallo-β-lactamases," J. Antimicrob. Chemother. **64**(3), 657–658 (2009).
11. X. Fan, I. M. White, S. I. Shopova, H. Zhu, J. D. Suter, and Y. Sun, "Sensitive optical biosensors for unlabeled targets: a review," Anal. Chim. Acta **620**(1-2), 8–26 (2008).
12. A. Ricciardi, A. Crescitelli, P. Vaiano, G. Quero, M. Consales, M. Pisco, E. Esposito, and A. Cusano, "Lab-on-fiber technology: a new vision for chemical and biological sensing," Analyst (Lond.) **140**(24), 8068–8079 (2015).
13. X. Chen, K. Zhou, L. Zhang, and I. Bennion, "Dual-peak long-period fiber gratings with enhanced refractive index sensitivity by finely tailored mode dispersion that uses the light cladding etching technique," Appl. Opt. **46**(4), 451–455 (2007).
14. P. Pilla, V. Malachovská, A. Borriello, A. Buosciolo, M. Giordano, L. Ambrosio, A. Cutolo, and A. Cusano, "Transition mode long period grating biosensor with functional multilayer coatings," Opt. Express **19**(2), 512–526 (2011).
15. P. Pilla, A. Sandomenico, V. Malachovská, A. Borriello, M. Giordano, A. Cutolo, M. Ruvo, and A. Cusano, "A protein-based biointerfacing route toward label-free immunoassays with long period gratings in transition mode," Biosens. Bioelectron. **31**(1), 486–491 (2012).
16. G. Quero, M. Consales, R. Severino, P. Vaiano, A. Boniello, A. Sandomenico, M. Ruvo, A. Borriello, L. Diodato, S. Zuppolini, M. Giordano, I. C. Nettore, C. Mazzarella, A. Colao, P. E. Macchia, F. Santorelli, A. Cutolo, and A. Cusano, "Long period fiber grating nano-optrode for cancer biomarker detection," Biosens. Bioelectron. **80**, 590–600 (2016).
17. G. Quero, S. Zuppolini, M. Consales, L. Diodato, P. Vaiano, A. Venturelli, M. Santucci, F. Spyrakis, M. P. Costi, M. Giordano, A. Borriello, A. Cutolo, and A. Cusano, "Long period fiber grating working in reflection mode as valuable biosensing platform for the detection of drug resistant bacteria," Sens. Actuators B Chem. **230**, 510–520 (2016).
18. D. Tondi, R. A. Powers, E. Caselli, M. C. Negri, J. Blazquez, M. P. Costi, and B. K. Shoichet, "Structure-Based Design and in-Parallel Synthesis of Inhibitors of AmpC β-Lactamase," Chem. Biol. **8**(6), 593–610 (2001).
19. R. A. Powers, J. Blazquez, G. S. Weston, M. I. Morosini, F. Baquero, and B. K. Shoichet, "The complexed structure and antimicrobial activity of a non-beta-lactam inhibitor of AmpC beta-lactamase," Protein Sci. **8**(11), 2330–2337 (1999).
20. R. A. Powers and B. K. Shoichet, "Structure-based approach for binding site identification on AmpC β-lactamase," J. Med. Chem. **45**(15), 3222–3234 (2002).
21. M. Minozzi, G. Lattanzi, R. Benz, M. P. Costi, A. Venturelli, and P. Carloni, "Permeation through the cell membrane of a boron-based β-lactamase inhibitor," PLoS One **6**(8), e23187 (2011).
22. P. Power, M. Galleni, J. A. Ayala, and G. Gutkind, "Biochemical and molecular characterization of three new variants of AmpC β-lactamases from *Morganella morganii*," Antimicrob. Agents Chemother. **50**(3), 962–967 (2006).
23. G. S. Weston, J. Blazquez, F. Baquero, and B. K. Shoichet, "Structure-Based Enhancement of Boronic Acid-Based Inhibitors of AmpC β-Lactamase," J. Med. Chem. **41**(23), 4577–4586 (1998).
24. I. Segel, *Enzyme kinetics: behaviour and analysis of rapid equilibrium and steady-state enzyme systems*, (Wiley Classic Library, 1993).
25. B. T. Burlingham and T. S. Widlanski, "An intuitive look at the relationship of K_i and IC50: a more general use for the dixon plot," J. Chem. Educ. **80**(2), 214 (2003).
26. W. L. Brooks and B. S. Sumerlin, "Synthesis and Applications of Boronic Acid-Containing Polymers: From Materials to Medicine," Chem. Rev. **116**(3), 1375–1397 (2016).
27. B. C. Das, P. Thapa, R. Karki, C. Schinke, S. Das, S. Kambhampati, S. K. Banerjee, P. Van Veldhuizen, A. Verma, L. M. Weiss, and T. Evans, "Boron chemicals in diagnosis and therapeutics," Future Med. Chem. **5**(6), 653–676 (2013).
28. Y. Chen, B. Shoichet, and R. Bonnet, "Structure, function, and inhibition along the reaction coordinate of CTX-M β-lactamases," J. Am. Chem. Soc. **127**(15), 5423–5434 (2005).
29. P. A. Kiener and S. G. Waley, "Reversible inhibitors of penicillinases," Biochem. J. **169**(1), 197–204 (1978).
30. D. Tondi, A. Venturelli, R. Bonnet, C. Pozzi, B. K. Shoichet, and M. P. Costi, "Targeting class A and C serine β-lactamases with a broad-spectrum boronic acid derivative," J. Med. Chem. **57**(12), 5449–5458 (2014).
31. X. Wang, G. Minasov, J. Blazquez, E. Caselli, F. Prati, and B. K. Shoichet, "Recognition and resistance in TEM β-lactamase," Biochemistry **42**(28), 8434–8444 (2003).
32. T. D. James, M. D. Phillips, and S. Shinkai, *Boronic acids in saccharide recognition*, Royal Society of Chemistry, (Cambridge, U.K., 2006).

Biomedical Optics EXPRESS

33. S. H. Lim, C. J. Musto, E. Park, W. Zhong, and K. S. Suslick, "A colorimetric sensor array for detection and identification of sugars," Org. Lett. **10**(20), 4405–4408 (2008).
34. K. C. Usher, L. C. Blaszczak, G. S. Weston, B. K. Shoichet, and S. J. Remington, "Three-dimensional structure of AmpC β-lactamase from *Escherichia coli* bound to a transition-state analogue: possible implications for the oxyanion hypothesis and for inhibitor design," Biochemistry **37**(46), 16082–16092 (1998).
35. S. B. Nimse, K. Song, M. D. Sonawane, D. R. Sayyed, and T. Kim, "Immobilization techniques for microarray: challenges and applications," Sensors (Basel) **14**(12), 22208–22229 (2014).
36. R. J. Davies, P. R. Edwards, H. J. Watts, C. R. Lowe, P. E. Buckle, D. Yeung, T. M. Kinning, and D. V. Polland-Knight, in *Techniques in protein Chemistry V*, (Academic Press, San Diego, CA, 1994), pp. 285–292.
37. M. J. Fischer, "Amine coupling through EDC/NHS: a practical approach," Methods Mol. Biol. **627**, 55–73 (2010).
38. F. Chiavaioli, P. Biswas, C. Trono, S. Bandyopadhyay, A. Giannetti, S. Tombelli, N. Basumallick, K. Dasgupta, and F. Baldini, "Towards sensitive label-free immunosensing by means of turn-around point long period fiber gratings," Biosens. Bioelectron. **60**, 305–310 (2014).

1. Introduction

The emergence of infections caused by Gram-negative resistant pathogens is rapidly and continuously increasing [1–3]. β-lactamases (BLs) are among the most diffuse resistance mechanism to β-lactams antibiotics such as penicillins and cephalosporins, being able to hydrolyze and consequently inactivate these drugs. For these enzymes β-lactam-based inhibitors such as clavulanic acid or sulbactam are ineffective and "β-lactamase stable" β-lactams, such as ceftazidime, are recognized as substrates. Indeed, some pathogens have evolved mechanisms that, in the presence of primary β-lactams or β-lactam-based inhibitor, up-regulate the expression of the BLs that they were designed to evade or inhibit. The broad activity of class C (AmpC) - BLs and the regulatory response to classic β-lactams has motivated a search for novel inhibitors structurally unrelated to β-lactams [4,5]. As researchers are struggling to find novel antibiotics and/or BLs inhibitors able to counteract resistance, new methods for BLs detection are increasingly necessary. The rapid identification of BLs produced by a pathogen and of the relative antibiotic resistance would, in fact, allow the administration of the most appropriate therapy and, possibly, the saving of last generation drugs, with a positive socio-economic impact on the whole society. The potential benefits of having an efficient BL detection system would include reduced hospitalization time, lower illness severity, lower treatment failure, and reduction in the escalation of antibiotic resistance in clinical settings and in the community. The methodologies currently available for the detection of BLs producing bacteria in biological samples generally require bacteria growing on Petri plates and resistance marker identification through the use of last generation antibiotics, BLs gene identification through PCR techniques or phenotypic approaches [6–10]. These methods are quite time consuming because of the necessary bacterial growth (about 24~48 hours according to the infecting bacteria), they are generally expensive, not always sensitive, and they also require trained personnel.

To overcome these limitations, label-free detection methodologies have been developed, since they allow the recognition of target molecules in their natural forms, and they are relatively easy and cheap. In this context, different highly sensitive optical probes, able to detect unlabeled biomolecules, have been developed [11,12]. Among all, Long Period Fiber Gratings (LPGs) are probably the most promising fiber grating technological platforms to be employed as label free biosensors, thanks to the intrinsic sensitivity to the surrounding refractive index (SRI) changes [11–16]. We recently developed a RT-LPG biosensor for the detection of drug resistance infection biomarkers [17]. Specifically, a standard LPG working in transmission mode was first transformed in a probe able to work in reflection configuration [16], and then coated with two polymeric overlays, atactic polystyrene (aPS) and polymethylmetacrylate-co-metacrylic acid (PMMA-co-MA), to maximize the device sensitivity in aqueous environments, and to provide the necessary conditions for a correct bio-functionalization. The well-known AmpC inhibitor 3-aminophenylboronic acid (3-APBA, compound **1**, Fig. 1) was first used as immobilized ligand on the RT-LPG surface [17], due its capability of binding AmpC with micromolar affinity (K_i = 7.3 μM) [18]. AmpC attachment

Biomedical Optics EXPRESS

tests on the biofunctionalized RT-LPG surface led to the protein detection at the very low concentration of 100 nM, in both purified and complex biological samples. Here we investigated the possibility of enhancing the performance of the aforementioned biosensor (reducing the LOD with respect to the previous one using 3-APBA) by using a different, more affine, boronic acid derivative. Specifically, using both structure-based [19,20] and transition-state analog approaches, several such novel ligands have been developed. Among the most potent of these there is benzo[b]thiophene-2-ylboronic acid (BZB, compound **2**, Fig. 1), which binds the canonical AmpC BLs with a K_i value of 0.027 μM [4]. More recently, Minozzi et al. [21] have identified 5-aminomethylbenzo[*b*]thiophen-2-boronic acid (BZD, compound **3**, Fig. 1) as a BZB's derivative with an improved permeability index, better solubility and better cell efficacy despite its higher K_i (0.26 μM).

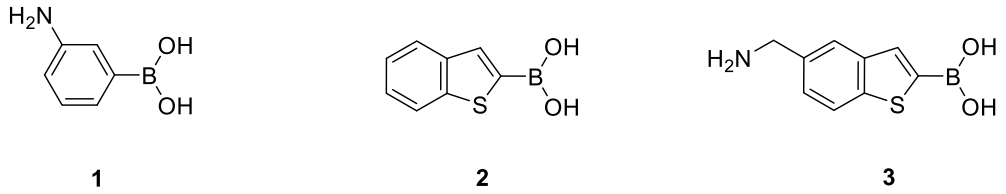

Fig. 1. Chemical structure of the selected AmpC boronic-based inhibitors: (**1**) 3-aminophenyl boronic acid (3-APBA), (**2**) benzo[b]thiophen-2-yl boronic acid (BZB) and (**3**) 5-aminomethylbenzo[b]thiophen-2-ylboronic acid (BZD).

Hence, among all the low nanomolar ligands developed, we finally decided to select BZD as a suitable ligand to fish out AmpC BL. The chemical and physical properties of BZD fulfill all the necessary requirements for the present study: the structure of BZD itself resembles that of BZB (one of the most known *in vivo* affine ligands for AmpC BL), the aminomethyl moiety in position 5 of its chemical structure behaves as a linker facilitating the binding on the double-coated RT-LPG surface. Hence, its solubility in buffer has been enhanced with respect to BZB and its inhibition constant (K_i) maintains a low value equal to 0.26 μM [4,21]. In this context, to perform simultaneous multi-target clinical analyses, we report the design and development of an automated system able to carry out both the immersion of different probes in several solutions (buffer, functionalizing and biological samples) and optical measurements. The results confirmed the capability of the RT-LPG biosensor to successfully monitor the presence of AmpC BL at a lower concentration and to obtain a sensitivity amplification of the device of a 2.96 factor. Also, the potential of the RT-LPG probe to specifically detect the β-lactams protein in complex matrices is reported.

2. Methods

2.1. Materials

Ethanol (EtOH), isopropyl alcohol (IPA, analytical grade 99.7), double-distilled water (ddH_2O), chloroform ($CHCl_3$, analytical grade 99.9), atactic polystyrene (aPS, MW = 280.000), poly(methylmethacrylate)-co-methacrylic acid (PMMA-co-MA, MW = 34.000), dextrose, aqueous ammonia (NH_3 30% w/w), 1-ethyl-3-[3-dimethylaminopropyl]carbodiimidehydro-chloride (EDC) and N-hydroxysuccinimide (NHS) were purchased from Sigma-Aldrich (Milan, Italy). Chloroform ($CHCl_3$) and potassium hydroxide (KOH) were purchased by J.T. Baker. 5-Aminomethylbenzo[*b*]thiophene-2-yl-boronic acid (BZD) were synthesized by reported procedure [4]. Recombinant AmpC BL was purified, and *Escherichia Coli* lysate solutions were prepared as reported below.

2.2. Protein purification and preparation procedure

AmpC BL of *Pseudomonas aeruginosa* was extracted from *E. Coli* BL21 (DE3) bacterial culture, carrying the pET9a_AmpC plasmid vector. The properly transforming bacterial cells,

Biomedical Optics EXPRESS

were selected by Ampicillin antibiotic resistance and then inoculated into 5.0 mL of Luria-Bertani (LB)-broth, at 37°C, 120 RPM, for 4 hours. The entire small-scale liquid culture was poured into 1.0 L of self-inducing growth medium and incubated at 37°C, 120 RPM, for 12 hours. The entire cell suspension was centrifuged at 4°C, 4500 RPM, for 40 minutes, recovering the bacterial pellet into the assay buffer solution (20 mM NaH_2PO_4, 30 mM NaCl, pH 7.5). The cells were broken by sonication cycles (Sonopuls HD 2070, Elettrofor) and the obtained sample was centrifuged at 4°C, 12000 RPM, for 30 minutes. The supernatant was recovered and filtered by 0.80-0.45 µm syringe filters. The resulting lysate sample was loaded onto XK 16/20 affinity column, functionalized with 3-methylaminophenyl-boronic acid (3-MAPB), previously equilibrated with the same assay buffer solution. AmpC target protein was purified using an automatic purifier system (AKTA Prime Instrument, Amersham Bioscience) and it was eluted by elution buffer (500 mM Boric Acid, 20 mM NaH_2PO_4, 30 mM NaCl, pH 7.5). BL enzyme activity was checked in each elution fraction by spectrophotometric method employing Cephalothin as β-lactam-antibiotic substrate at final concentration of 100 µM. The most active fractions were pooled together, in order to have a final concentration of 1 mg/mL, as assessed by UV-scan assay. The purity grade of the purified protein sample was checked by SDS-page analysis (>> 95%). The protein sample was lyophilized and a proper protein-reconstitution protocol has been set up, in order to obtain AmpC protein solutions at fixed concentration for the next binding experiments. The so reconstituted AmpC BL was then added into the cell lysate samples obtaining a final calculated BL concentration equal to 3.65 µM [17].

2.3. AmpC BL kinetic assay

The full kinetic profile of purified AmpC BL was evaluated measuring the experimental values of the parameters mainly describing the kinetic activity of the enzyme protein (catalytic constant kcat and substrates-affinity constant Km). The experimental results, for each parameter, were in agreement with the data reported by the scientific literature [22]. In order to assess the kinetic functionality of the purified AmpC protein, we have performed a kinetic assay by spectrophotometric method (DU-640 spectrophotometer, Beckman Coulter). The assay consists of monitoring the time-dependence β-lactam hydrolysis enzyme reaction, at the specific wavelength of the Cephalothin antibiotic substrate (265 nm), for a total time of 300 seconds. The kinetic assay was performed at room temperature (RT), in a final total volume of 600 µL. The several reaction reagents were properly added as followed: 1) assay buffer solution to volume of 600 µL (20 mM NaH_2PO_4, 30 mM NaCl, pH 7.5); 2) AmpC enzyme at concentration of 0.115 µM; 3) Cephalothin β-lactam antibiotic substrate at final concentration value of 100 µM. The third step represents the rate-determining step (RDS), because the adding of antibiotic substrate causes the starting of the enzyme reaction. The resulting V_{max} value equal to 0.235 µM/s, confirmed the acceptable kinetic rate of the AmpC enzyme under the considered experimental conditions.

2.4. Enzymatic inhibition assay

The capability of BZD compound for binding and inhibiting the kinetic activity of the AmpC enzyme, was evaluated by detecting the IC_{50} (the inhibitor's concentration able to reduce by 50% the enzyme activity of AmpC BL). The assay consists of evaluating, by spectrophotometric method at the specific Cephalothin absorption wavelength (265 nm) for 300 seconds, the dose-dependence reduction of enzyme kinetic activity with increasing concentrations of inhibitor molecule. With this aim, the assay is performed at fixed value of enzyme and substrate concentration, varying the concentration of the inhibitor. The compound was first dissolved in dimethyl sulfoxide (DMSO) in order to obtain an initial concentration of 10 mM. First, an inhibition assay at two single concentration points (0.25 and 0.50 µM), in duplicate, was performed to identify the optimal ligand concentrations range for the next IC_{50} assay. Based on the obtained inhibition data (19% and 41% respectively), the

Biomedical Optics EXPRESS

ligand IC_{50} value was evaluated by testing six different concentrations (0-0.1-0.2-0.4-0.8-1.6 µM) and using an enzyme and a substrate concentration of 0.115 µM and 100 µM, respectively. Each inhibitor concentration was analyzed in duplicate with a statistical significance (*p-value* < 0.005). Assuming a competitive inhibition for the BZD compound, like other boron-based non β-lactam inhibitors [23], it is possible to calculate the IC_{50} value from the plot 1/V vs [I] considering the general equation $IC_{50} = \{[(1/2V_{max/}) - q]/m\}$ [24]. In this way, the IC_{50} value for the BZD inhibitor was equal to 0.75 µM. In good approximation, regarding the competitive inhibitors, the IC_{50} is correlated to the inhibition constant value (K_i) using the Cheng-Prusoff relationship ($IC_{50} = K_i [1 + ([S]/Km)]$) [25]. The corresponding K_i value for the BZD compound (0.23 µM), was in agreement with the value previously reported in literature (0.26 µM) [4].

2.5 Preparation of reflection-type LPG probe and surface biofunctionalization

The main *fabrication* steps for the realization of the RT-LPG are (i) the inscription of the grating in the optical fiber followed by the fiber cutting, (ii) the Ag reflecting layer (i.e. the mirror) integration on the fiber tip and (iii) the double layer (aPS and PMMA-co-MA) deposition on the RT-LPG surface. All steps were performed following the procedures reported in Ref. 17.

The sensor surface *biofunctionalization* is composed of two steps: (i) the activation of the carboxylic groups by EDC/NHS reaction and (ii) the BZD ligand anchoring onto the RT-LPG biosensor surface. The activation of the carboxylic groups is made possible by a first immersion of the probe in 1.0 mL of clean ddH_2O followed by addition of 0.5 mL of a freshly prepared EDC/NHS solution (0.05 M/0.03 M, 1:1 molar ratio) and by a final washing in ddH_2O (30 min). Once the activation of the carboxylic groups is performed, the BZD anchoring can be achieved through the sequential immersion in: ddH_2O (30 min), 3.38 mM BZD solution (60 min) and, again, ddH_2O (30 min). To ensure the most possible coverage, the BZD anchoring procedure was repeated twice. The so functionalized RT-LPG probe was used for the following protein binding tests.

2.6. Protein binding test

On the BZD-functionalized RT-LPG, tests were performed using AmpC BL solutions at different increasing concentrations, in the range of 50-500 nM. The procedure consisted of sequential immersions of the probe in solutions [17] and for each AmpC concentration tested the steps are: (i) washing in ddH_2O, (ii) immersion in AmpC solution, and (iii) washing in ddH_2O.

3. Results and discussion

3.1 The new ligand (BZD)

In this paper we used as probe BZD that has a different biological profile with respect to 3-APBA studied in our previous work [17]. BZD is also able to inhibit the AmpC enzyme, but it is about 30 times more active with respect to 3-APBA [26,27]. This difference in K_i (0.26 µM with respect to 7.3 µM) might lead to a different performance of the device upon the ligand attachment, worthy of being investigated. In principle, we expected that the higher affinity of BZD for AmpC could lead to a higher efficiency in capturing the enzyme (ligand-protein complex formation) from the cytoplasmic environment, and to a higher specificity generating less background noise in the device detection signal.

3.2 Design and development of the automated system for simultaneous multi-target clinical analyses

As known, a typical molecule/protein detection test, involving a RT-LPG probe, requires the immersion of the transducer in a variety of solutions used to functionalize the surface of the

Biomedical Optics EXPRESS

probe and reveal the concentration of the target analytes. These stages are interspersed by the immersion of the probe in several buffer solutions, depending on the specific kind of experiment. Therefore, it becomes essential to provide an automatic positioning system allowing the immersion and extraction of the sensor within the different liquid solutions. Another fundamental requirement is the ability to process more RT-LPG probes simultaneously, enabling the testing of different kind of solutions (e.g., detecting the presence of different classes of BL using distinct protocols of functionalization) at the same time, resulting in a higher throughput. In order to address these needs, we have designed and developed an automated system able to fully operate up to eight RT-LPG probes in specific protocols, by changing the solutions under test and performing optical measurements.

The design of the system addresses two different requirements: i) it features a set of electrical and mechanical components concerning the movements required to change the solutions during the experiments; ii) it is provided with an optoelectronic unit related to the optical interrogation of the RT-LPG probes. The system has been designed using Solid Works (Dassault Systemes SolidWorks Corporation), a 3D mechanical CAD (computer-aided design) software. Figure 2 shows a conceptual scheme summarizing the main parts of the system. Essentially, a support (*fiber holder*) holds up eight optical fibers, in such a way that the terminal part of them (*sensing tips*) is disposed vertically, and parallel to the others. In this way, the sensitive end of each probe, namely the RT-LPG, is aligned with the centre of the cuvettes in which it will be immersed, avoiding any contacts with the walls of the cuvettes themselves.

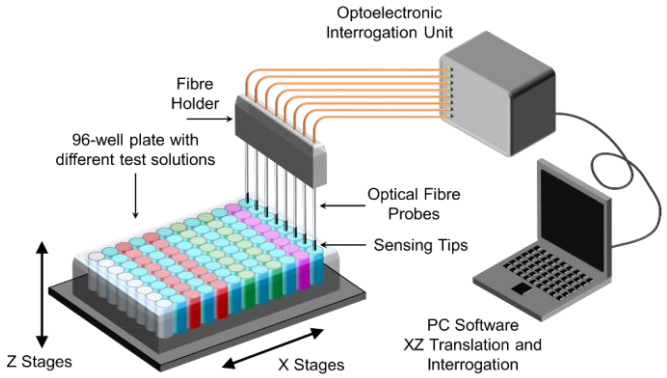

Fig. 2. Conceptual scheme summarizing the main parts of the system.

The automatic change of the solutions is realized by translating a cuvette carousel sustaining a standard 96-well plate (providing a matrix of 12 × 8 cuvettes), through the control of two linear actuators along the horizontal (X) and vertical (Z) directions. Although different configurations could be considered, it is preferable to move only the cuvette carousel, keeping the fibre probes fixed during all the operations, avoiding any power fluctuations throughout the experiments. A customized optoelectronic processing unit collects the spectra of the eight RT-LPG probes. A PC software manages both the movements and the spectral interrogation, retrieving and elaborating the optical probes outputs.

All the components have been integrated into a suitable enclosure, protecting all the delicate parts on its inside, including the RT-LPG probes, the 96-well plate, the linear actuators, the optical components and the electronic circuitry. A door provides access to the test chamber (see Fig. 3(a)), where it is possible: i) to mount the transducers, through a delicate but precise fixing, assisted by a small CMOS camera (HP Webcam HD 5210, HP Development Company, L.P., CA, USA) connected to the PC; ii) to fill the cuvettes with liquid solutions required by the protocol. The 96-well plate (available with different heights and volumes of hundreds of µL from Corning Enterprises, Corning, NY, USA) is held by a

Biomedical Optics EXPRESS

plate moved by the vertical linear actuator (DL 20-45-ST-PH from Del-Tron Precision, Inc., CT, USA), which allows to immerse and withdraw the RT-LPG probes into the cuvettes. The vertical actuator is mounted on the horizontal one (BG 2602A-200P/A5K from Nippon Bearing Co., LTD, Japan), which moves along the X direction, translating with itself the vertical actuator and the 96-well plate.

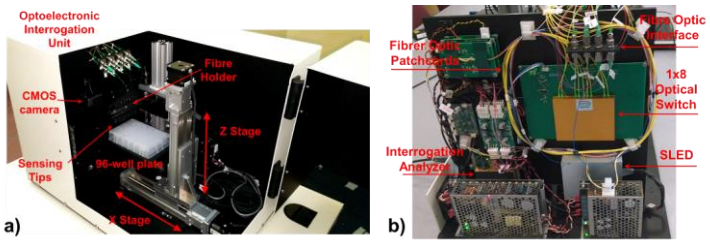

Fig. 3. (a) View of the manufactured automated system, showing the test chamber. (b) View of the optoelectronic interrogation unit and electronic circuits hosted on the side panel (the enclosure has been removed).

The optoelectronic interrogation unit, the electronic circuits for the control of the entire system, the connection with the host PC and the power supply are mounted on a side panel, as shown in Fig. 3(b) (where the enclosure has been removed). The optoelectronic interrogation unit is schematically shown in Fig. 4. Basically, a light source (SLED, Superluminescent Light Emitting Diode, peak wavelength = 1575.98 nm) illuminates the RT-LPG probes, whose reflected spectra are sent every 45 seconds to a spectrometer (WaveCapture™ Spectrometer, BaySpec, Inc, CA, USA), characterized by a wavelength range of 80 nm (1530-1610 nm), an absolute wavelength accuracy of ± 35 pm and a wavelength repeatability of 5 pm.

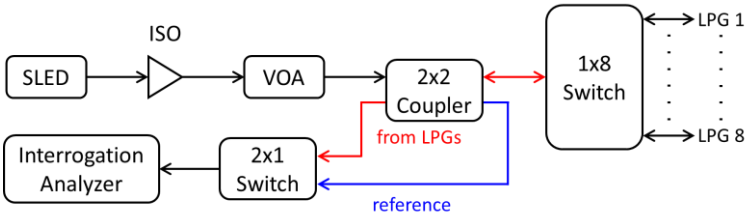

Fig. 4. A scheme of the architecture of the optoelectronic interrogation unit.

An optical isolator (ISO) is inserted just after the light source, allowing the transmission of light in only one direction, avoiding undesirable feedback into the source. A variable optical attenuator (VOA) ensures proper control of the power intensity emitted by the source preventing the saturation of the spectrum. A 1x8 optical switch is used to select and interrogate one at a time each RT-LPG probe. In order to obtain normalized spectra (C), a 2x2 coupler and a 2x1 switch are used. In particular, we first acquired the reference spectrum of the light source itself (A, blue path in Fig. 4), then we acquired the spectra reflected by the RT-LPG probes (B, red path in Fig. 4). Once the spectra have been acquired, a software (Sense 20/20, BaySpec, Inc, CA, USA) adequately customized performs a normalization following the equation shown below Eq. (1):

$$C(\lambda) = 10 \times \mathrm{Log}_{10}\left[B(\lambda) / A(\lambda)\right]. \quad (1)$$

Then the spectra are filtered and elaborated providing the central resonance wavelengths (λ_c) of each spectrum, enabling a continuous and real time monitoring of the interaction kinetics of the biological molecules on the RT-LPG surface. Moreover, to perform completely

Biomedical Optics EXPRESS

automated biological tests, the customized software allows to execute automated scripts, including the commands for the translation stages and acquisition of the RT-LPG spectra.

3.3 Experimental results

Since boronic acid-derivatives are high affinity inhibitors of BLs [28–31], in our previous work the well-known AmpC inhibitor 3-APBA was immobilized on the RT-LPG surface, and used to bind and recognize AmpC in both purified solutions and complex biological samples, at the very low concentration of 100 nM. These encouraging results induced us to verify, and possibly improve, the capability of the RT-LPG biosensor to detect AmpC presence using a different boronic-acid derivative. The BZD ligand was selected according to the following properties: the predicted orientation within the enzyme binding site (as described below) and the high affinity towards the target AmpC BL [17]. Furthermore, BZD fulfills the bioanchoring requirement, having a primary amine able to covalently bind the ester groups that functionalize the double-coated RT-LPG surface.

3.3.1 Inhibition activity of boronic acid against AmpC BL

The typical reactivity of the boronic group is due to its empty orbitals on the boron atom and its susceptibility to react with nucleophiles as the active site serine of BLs. The diols formation due to dehydration reaction with sugar hydroxyls gives rapidly reversible diols and therefore these compounds are used for the recognition of sugars derivatives in analytical device [32,33]. The BLs inhibition mechanism of phenyl and benzothiophene boronic acid derivatives is based on the formation of a reversible covalent acyl-enzime intermediate with the BL enzyme [17]. These compounds, in fact, mimic the antibiotic transition state, with the boronic group replacing the β-lactam ring and interacting with the catalytic serine through the formation of a similar tetrahedral intermediate (Fig. 5(a)). A necessary condition for the interaction and recognition of BLs is that the boronic group is free to interact with the hydroxyl moiety of the enzyme catalytic site represented by a serine molecule. The boronic group represents the chemical recognition element fundamental for the covalent bond formation. The ligand has to bear a primary amino group for anchoring to the RT-LPG probe.

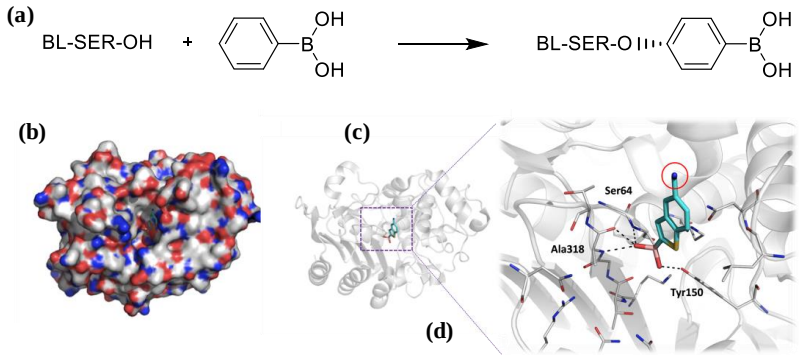

Fig. 5. (a) Action mechanism of a generic boronic acid inhibitor. (b-d) Possible orientation of BZD in AmpC binding site (derived by AmpC-BZD complex; PDB code 2i72 [35]). Overall view of the BZD-AmpC BL complex (b) and (c). The protein is represented as surface and cartoons, respectively, the ligand in capped sticks. (d) Binding site close-up. BZD and the residues lining the pocket are shown in capped sticks. Hydrogen bonds formed by the ligand with the surrounding residues are reported as black dashed lines. Crucial residues are labelled. The amino group involved in the RT-LPG covalent anchoring is highlighted by the red circle.

The binding mode of BZD in AmpC binding site is reported in Fig. 5(b)-5(d). The BZD-AmpC complex was modelled on the x-ray AmpC-5-diformylaminomethyl-benzo[b]thiophen-2-boronic acid complex (PDB code 2i72) [34], upon deletion of the diformyl moiety. The ligand is able to covalently bind to the catalytic Ser64 through the

Biomedical Optics EXPRESS

boronic group and to form hydrogen bonds with the same Ser64, the Ala318 backbone, and the Tyr150 side chain, thus stabilizing the complex formation. The amino group shows a relevant accessible surface area and is not directly involved in any contact with the surrounding residues (while 3-APBA forms a hydrogen bond with Asn346 [34]. The space availability around the primary amine suggests that the anchoring process, involving the formation of a covalent bond between the amino group and the ester moieties on the RT-LPG surface, would not dramatically affect the structural organization of the AmpC-BZD complex. Nevertheless, the immobilization of the ligand on the fibre surface and the consequent reduction of the ligand degrees of freedom, the presence of an additional amidic bond, and the loss of the primary amino function might reasonably change the value of the estimated K_i for the protein-ligand complex in solution.

3.3.2. Biofunctionalization of RT-LPG

Among several methods generally used for the biofunctionalization of probes on solid surface, an attractive strategy is represented by the covalent attachment of ligands causing an improvement in terms of reliability, selectivity and sustainability [35]. The adopted standard procedure consists of the preparation of a succinimidyl ester (-COOSuc)-terminated surface layer through the reaction with N-hydroxysuccinimide (NHS), in the presence of a water-soluble carbodiimide as N-ethyl-N'-(3-dimethylaminopropyl)-carbodiimide (EDC) or other similar coupling agents [36,37]. In particular, the activated amine-reactive esters, easily form covalent bonds with the BZD ligand. Hence, the binding of BL protein can occur due to the affinity for the ligand on the surface.

A generic BZD binding experiment consists of a first activation of the carboxyl groups on the sensor surface by treatment with EDC/NHS and by the successive reaction with BZD. In Fig. 6(a) the typical real time sensorgram, reporting the time variation of the probe resonance wavelength obtained during the biofunctionalization of the RT-LPG transducer is showed. The RT-LPG was immersed in 1.0 mL of ddH_2O (step **I**) to acclimate the sensor surface and rinsed until the stabilization of the optical signal (for about 45 min) and, subsequently, 0.5 mL of EDC/NHS solution were added dropwise (step **II**), to reach respectively 0.05/0.03 M (1:1) concentrations in the final solution. Then, the sensor was rinsed in 1.5 mL of clean ddH_2O (step **III**), for about 30 min, to remove the reagent non-specifically bound to the sensor surface. The RT-LPG resonance wavelength shift recorded between steps III and I ($\Delta\lambda_{III-I}$), and due to the activation of the carboxylic groups on the PMMA-co-MA surface, was about –2.0 nm. The so activated sensor surface was then immersed in 1.5 mL of BZD solution (step **IV**) and the kinetic of covalent binding was monitored for a reasonable time of 60 min followed by washing in clean ddH_2O (step **V**). The ligand was used in excess to guarantee the highest possible surface coverage of carboxyl groups on PMMA-co-MA layer per immersion step. Between the two washing steps (steps V and III), a blue shift $\Delta\lambda_{V-III} = -1.2$ nm was observed for the optical signal indicating the BZD attachment to the surface. The ligand binding was repeated (**VI** and **VII**) in the same conditions to ensure a complete coverage of all the surface functionalized groups. The wavelength shifts recorded (steps VII and V) were $\Delta\lambda_{VII-V} = -1.8$ nm. As expected, the interaction of BZD with the sensor surface- induces a decrease of the output signal, which can be explained with an increase of the thickness of the deposited biolayer.

3.3.3. AmpC BL detection

The optical biosensor capability of binding AmpC was subsequently tested on a wide range of protein concentrations (50 nM - 5.0 μM). Figure 6(b) reports the real time sensorgram obtained with three increasing AmpC concentrations of 50, 100 and 300 nM, respectively. The BZD-coated RT-LPG was immersed in clean ddH_2O (**VIII**) for a first acclimation. After the stabilization of the optical signal, the RT-LPG probe was extracted and successively immersed in an AmpC BL solution at the low concentration of 50 nM (**IX**), until the

Biomedical Optics EXPRESS

stabilization of the optical signal (about 60 min). The molecules non-specifically bound on the sensor surface were removed by washing the probe in ddH_2O (**X**). The wavelength shift recorded between the two washings (steps X and VIII**)** was equal to –0.45 nm. These last steps, i.e. the immersion in a fresh protein solution followed by the washing in ddH_2O, were repeated in the same conditions using higher AmpC concentrations, that is, 100 and 300 nM (steps **XI-XIV**). The measured wavelength shifts (between the washings before and after the AmpC binding) turned out to be –0.75 and –1.95 nm, respectively. Then, the saturation grade of the biofunctionalized surface of the RT-LPG biosensor, also at higher AmpC concentrations (0.5, 1.0 and 5.0 μM) were explored. In these cases, the $\Delta\lambda_{AmpC\text{-}binding}$ resulted, respectively, –2.40, –0.50 and –0.15 nm. In Fig. 6(c) is reported a schematic representation of the RT-LPG coated with aPS and PMMA-co-MA layers after AmpC BL binding experiments.

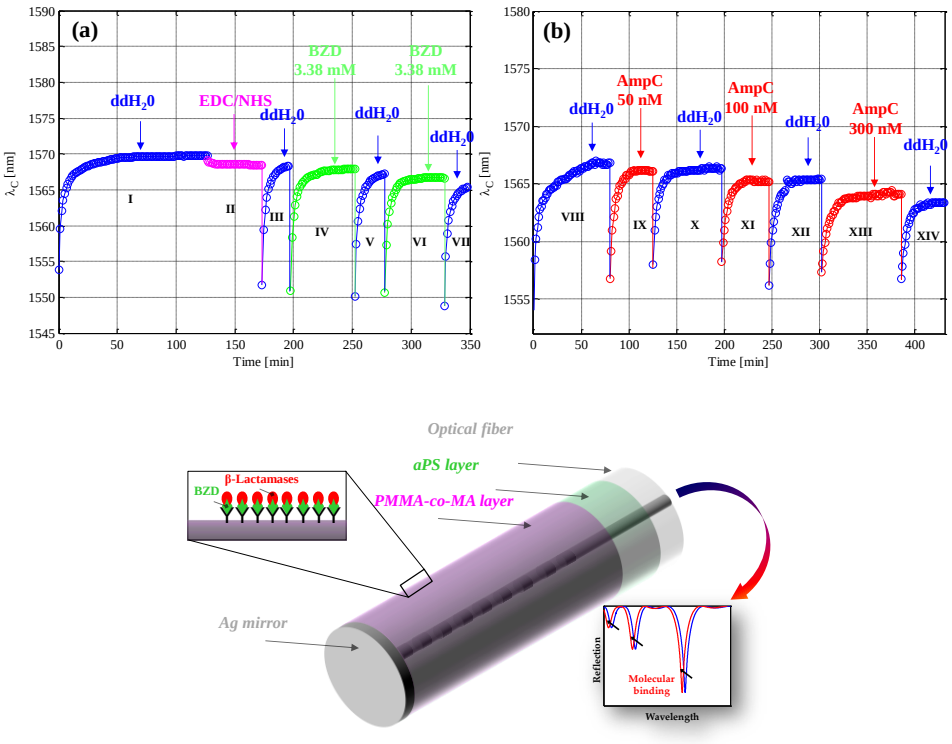

Fig. 6. (a) RT-LPG sensorgram during the biofunctionalization phase. (b) RT-LPG sensorgram during the AmpC β-lactamase binding experiments. (c) Schematic representation of the RT-LPG coated with aPS and PMMA-co-MA layers for AmpC β-lactamase binding experiments.

It is worth mentioning that the time actually needed for the protein binding test comprises only the three steps reported in section 2.6: (i) washing in ddH_2O, (ii) immersion in AmpC solution, and (iii) washing in ddH_2O, while the previous steps can be considered as preparation steps, not affecting the effective time required by the protein detection. Therefore, assuming the LPG sensor ready for the detection, the total time required for the analysis using the proposed LPG probes is about 150-200 min. This quite long response time exhibited by the LPG probe is mainly due to the uptake time required to stabilize the coated LPG when used in batch tests. Indeed, every time the LPG probe is extracted and submerged into a new solution, a sort of acclimatization of the polymer layer is observed as a fast red wavelength shift [14–17] (lasting ~30 min) before the RT-LPG biosensor response reaches a steady state

Biomedical Optics EXPRESS

value. However, we wish to point out that the integration of the RT-LPG platform in a suitable optofluidic system, enabling its operation in flow condition, would enable to avoid the LPGs extraction/submersion into the aqueous solutions and, consequently, the uptake process, leading to a significant reduction of the biosensor response time [38]. A correct analysis of the recorded measures requires to consider the following issue: although the fabrication process is robust and repeatable, a normalization procedure is needed to account for the even tiny discrepancy in the SRI sensitivities of different RT-LPG probes (mainly due to the LPG fabrication tolerances or to slightly different aPS or PMMA-co-MA overlay thickness obtained in the different devices). To this aim, we performed a normalization between the wavelength shift ($\Delta\lambda_{air\text{-}water}$) occurred in two medium with different refractive index (SRI_{air} = 1 and SRI_{water} = 1.333) and the wavelength shift occurred upon PMMA-co-MA layer deposition ($\Delta\lambda_{PMMA}$). Then, we defined an observable as:

$$O_{air-water} = \Delta\lambda_{air-water} / \Delta\lambda_{PMMA}$$

The normalized value ($O_{air\text{-}water}$) for the probes used in the experiments is very similar ($O_{air\text{-}water}$ mean value is 6.5 with a RSD of 6%) and guarantees good robustness and reliability. In line with this argument, considering that the ligand or protein binding has been calculated as the wavelength shift after and before washing in water, we defined a new observable as:

$$O = \Delta\lambda_C / \Delta\lambda_{PMMA}$$

where, $\Delta\lambda_C$ corresponds to the wavelength shift after and before washing in water. This method allows the comparison of the results obtained with different RT-LPG probes, and built up a unique biosensor AmpC dose-response curve (i.e. the biosensor calibration curve).

The obtained curve (orange curve in Fig. 7) presents a linear behavior at low AmpC concentrations (50 - 300 nM), while it reaches the saturation for higher protein concentrations.

To monitor the non-specific protein binding, a blank test has been also performed using a coated RT-LPG previously treated with only EDC/NHS (without anchoring the BZD ligand). The purified AmpC was tested using the same procedure and increasing the protein concentration. No sensor response was registered at low concentrations, while a slight blue shift ($\Delta\lambda$ = –0.08 nm) was measured starting from 1.5 µM concentration (cyan curve in Fig. 7), which, however, turned out to be more than seven times lower with respect to the response obtained with the biofunctionalized device. The results confirmed the high affinity of the BZD ligand and, overall, the potentiality of the proposed bioprobe.

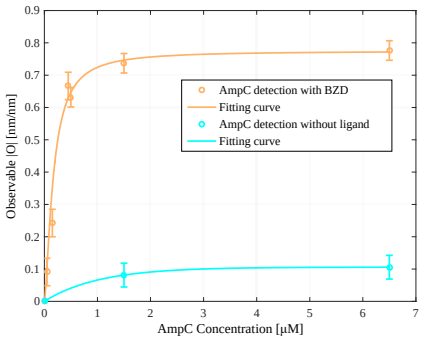

Fig. 7. Characteristic curves (O vs. AmpC BL cumulative concentrations) of the RT-LPG device obtained by binding experiments with purified AmpC (orange curve) and negative blank test using not functionalized probe (cyan curve). The error bars refer to the standard deviation calculated by considering the results obtained by repeating 3 times the experiment with the same concentration.

Biomedical Optics EXPRESS

In order to roughly estimate the limit of detection (LOD) of the BZD-functionalized RT-LPG biosensor, we determined the sensitivity against AmpC BL, calculated as the derivative of the characteristic curve (O vs. AmpC concentration) in the linear region (50-300 nM):

$$S_{AmpC-BZD} = \partial O_{AmpC-BZD} / \partial C = 1.449\ \mu M^{-1} \quad (1)$$

Considering that the minimum observable O_{min} can be expressed as:

$$O_{min} = \Delta\lambda_{min} / \Delta\lambda_{PMMA} \quad (2)$$

where $\Delta\lambda_{min}$ is the minimum wavelength variation (set by the interrogation unit) and equal to 35 pm, the LOD for the probe functionalized with BZD resulted:

$$LOD_{AmpC-BZD} = O_{min} / S_{AmpC-BZD} \approx 6\ nM$$

3.3.4. AmpC BL detection in bacterial lysate solution

Once verified the effectiveness of the BZD-coated RT-LPG biosensor in purified AmpC samples in PBS buffer solutions, we were interested into detection of BL at low concentrations - which are more important in biomedical field - in more complex biological models. Hence, further experiments were carried out to investigate the bioprobe capability to detect the presence of protein in bacterial lysate samples, in which AmpC was previously added. For this purpose, *E. Coli* lysates were used with AmpC at 50 nM and 100 nM concentrations. A representative sensorgram obtained during the tests in "lysate" is reported in Fig. 8(a). Similarly to the previously reported procedure, the biofunctionalized RT-LPG probe was first acclimated in clean ddH_2O (**VIII'**), and successively immersed for about 60 minutes in the lysate sample (**IX'**) containing an AmpC BL concentration of 50 nM. Finally, the probe was washed in clean ddH_2O (**X'**) to remove the molecules non-specifically bound to the sensor surface. The RT-LPG probe was also tested with a further, slightly higher, AmpC BL concentration of 100 nM (**XI'**), followed by rinsing in ddH_2O for about 60 minutes (**XII'**). Although the low BLs concentrations used in this test (i.e. 50 nM and 100 nM), the wavelength shifts ($\Delta\lambda_{C\_Lys}$) recorded by our device between **X'** and **VIII'** steps, and between **X'** and **XII'** steps resulted to be as high as –0.5 nm and –1.0 nm, respectively. The calculated values of the observable O corresponding to AmpC concentrations detected in complex lysate (violet stars) resulted to be in perfect agreement with the one obtained for purified AmpC in PBS buffer solutions (orange curve in Fig. 8(b), 8(c)). Control experiments to verify the possible effect of the complex matrix in the detection of lower protein concentrations were also performed. In particular, a RT-LPG probe previously treated with only EDC/NHS, (without anchoring the BZD ligand) was tested in a lysate solution.

Biomedical Optics EXPRESS

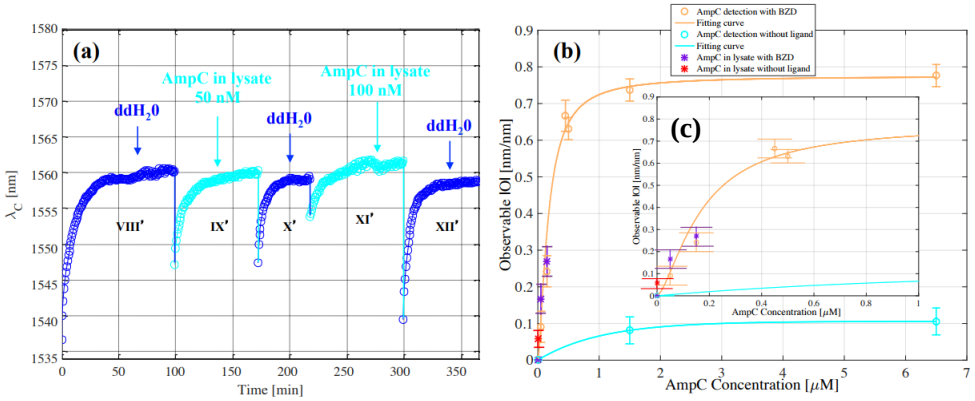

Fig. 8. (a) Reflection-type LPG sensorgram reporting the central wavelength shift of 6th cladding mode attenuation band during the AmpC BL binding for lysate solutions containing different protein concentration. (b) Characteristic curves (O vs. AmpC BL cumulative concentrations) of the RT-LPG device obtained for binding experiments with purified AmpC (orange curve) in PBS buffer solution and AmpC in complex lysate (violet stars), negative blank test (i.e. using not functionalized probes) in PBS buffer solution (cyan curve), and control test using complex lysate without BZD (red star). The error bars refer to the standard deviation calculated by considering the results obtained by repeating 3 times the experiment with the same concentration. (c) Inset showing a magnification of the results obtained at low concentrations.

The results reported as red star in Fig. 8(b) showed a very small response both in terms of resonance wavelength variation ($\Delta\lambda_{Lys\_blank} \cong 0.35$ nm) and observable (O ≅ 0.058). The observable value resulted to be less than half the value obtained when the lysate solution contained 50 nM of AmpC BL, thus confirming once more the capability of our device to correctly detect the target protein also in complex media.

As mentioned at beginning of the paper, our first experiments on RT-LPG biosensor were performed using 3-APBA, a commercial product previously applied for AmpC BL detection in colorimetric assays. 3-APBA, due to low cost and low micromolar affinity towards β-lactamase, represented the best option for our first experiments, necessary to test the proof of principle related to RT-LPG biosensor based on small molecule ligands as bio-receptor. Non-commercial ligands with different chemical and biological features were then selected to improve the system applicability and enhance the innovation aspects of the detection system. BZD was selected among boronic acids due to its about 30-fold higher affinity towords AmpC with respect to the previously tested 3-APBA, with K_i being 0.26 and 7.3 μM, respectively. To verify the RT-LPG biosensor performance improvement, we compared in Fig. 8(b) the calibration curves with those obtained by using the 3-APBA-functionalized RT-LPG, and observed that: i) the presence (common to both biosensors typology) of a linear region in a low concentration range (up to 300-500 nM) and a saturation region where a plateau value (over about 3.0 μM) was achieved; ii) the sensitivity of the RT-LPG probes functionalized with the BZD (i.e. the slope of the calibration curve in the linear region) is much higher (1.449 μM^{-1}) with respect to that provided by the 3-APBA-based device (0.486 μM^{-1}), and this results in a reduction of the LOD of the former device of a factor higher than three (6 nM instead of 20 nM); iii) both biosensors exhibit a saturation regime in correspondence of an O value of about 0.8. Overall, the results here reported confirm the potentiality of the RT-LPG fiber optic biosensing platforms, which enables to correctly detect AmpC BL at low nM concentration, even in complex biological matrix as bacterial lysate.

4. Conclusions

We reported here a valuable proof of principle for the development of fully automatic optical assays for the real time monitoring of AmpC BLs, one of the most important source of

Biomedical Optics EXPRESS

resistance to BL antibiotics expressed by drug resistant bacteria. Highly sensitive fibre optic optrodes based on LPG working in transition mode and operating in reflection were selected as enabling technologies for the automatic assay. As probes, boronic acids were selected in light of their BL inhibition capability and among them, BZD was judiciously identified to be covalently bound to the sensor surface due to its enhanced affinity for AmpC BL with respect to the previously used 3-APBA. Furthermore, the selected probe presents a favorable orientation within the protein binding site allowing a better anchoring reaction and, thus, a more effective probe functionalization. In order to provide an engineered platform for automatic optical assays, a dedicated opto-bio-lab system has been developed including an automatic positioning system able to simultaneously manipulate eight RT-LPG probes during all the specific phases of the assay. The system also includes the optical readout for the real time monitoring of the optical fibre biosensors though spectral analysis. A wide set of AmpC BL binding tests was performed using RT-LPGs functionalized with BZD on samples containing the purified target protein at increasing concentrations in the 50 nM - 5.0 μM range. Overall, the reported results clearly demonstrated the capability of the developed optical biosensor to correctly perform the label-free detection of AmpC BLs, both in simple and complex biological samples. Dose-dependent experiments showed that the sensor response is linearly dependent to the protein concentrations in the low-concentration range. The results here obtained for BZD demonstrated a LOD of about 6 nM, three times lower than that obtained using the same RT-LPG platform functionalized with a lower affinity ligand (3-APBA).

Funding

EU Project “Multianalyte automatic system for the detection of drug resistant bacteria - OPTObacteria” (Project reference: 286998).

Disclosures

The authors declare that there are no conflicts of interest related to this article.